LES OF A RECTANGULAR BUBBLE COLUMN

Knut Bech

SINTEF Materials and Chemistry, 7465 Trondheim, NORWAY

ABSTRACT

Large-eddy simulation of a rectangular bubble column was carried out at two different meshes and with two different models for the relative velocity between liquid and gas. The results were compared to simulations applying the $k\omega$ and $k\epsilon$ turbulence models, as well as 2D simulations and experimental data from literature. The transient plume behavior predicted with the LES and the $k\omega$ models resemble experimental results, while the regular plume oscillation observed with the $k\epsilon$ model is different from experimental observation. The effort involved in constructing phase averages of the flow field turned out to be considerable, probably due to a lack of perfect periodicity in the plume oscillation, as well as high frequency motion.

INTRODUCTION

The meandering, or oscillating, plume that occurs in a rectangular bubble column at certain gas flow rates has been the subject of several computational studies. The flow pattern is depicted in figure 1. A review of literature and a discussion of two-dimensional (2D) simulations can be found in Bech (2005). The present paper discusses results on 3D simulations, notably Large Eddy Simulation (LES), but with additional simulations applying two-equation dynamic turbulence models. In literature, the $k\epsilon$ turbulence model has been the common choice, see for example Becker et al. (1994), Sokolichin and Eigenberger (1999), Pfleger and Becker (2001), Buwa and Ranade (2002), Troshko and Hassan (2001), Oey et al. (2003). A statement common for many of these papers, is that only 3D simulations can reproduce the transient behavior of meandering plume. As discussed by Bech (2005), this failure to reproduce the transient motion is due to the turbulence model, not the dimensionality of the simulation. In the present investigation, the $k\omega$) turbulence model is applied for comparison. The application of the LES method on multiphase flow simulations of bubble columns has been reported by Deen et al. (2001), on a square cross-sectioned column, and by Takeda et al. (2004) on circular columns. Deen et al. (2001) reported that the simulated plume was steady when applying the $k\epsilon$ model, but exhibited a transient behavior when the LES model was applied. The LES model was in good quantitative agreement with experimental results. The results showed some grid-dependence, especially near the column side walls.

The geometry of the case to be discussed in the present paper is given in figure 2, and corresponds to the configuration applied by Pfleger et al. (1999) and Buwa and Ranade (2002). The superficial gas velocity was 0.167 cm/s, and the sparger area was $1.08 \cdot 10^{-4}$ m². This paper will present results on the period of oscillation and the mean velocity. Detailed analysis of the turbulence field was out of scope due to limited time.

THEORY

The theory is described in detail in Bech (2005). In the present work, descriptions of the relative velocity and the sub-grid scale viscosity have been added.

Governing equations

The continuity equation is

$$\frac{\partial \rho}{\partial t} + \frac{\partial}{\partial x_j}\left(\rho u_j\right) = 0 \qquad (1)$$

Here, ρ is the mixture density to be defined below, and u_j is the j-component of the mixture velocity. The conservation equation for the disperse volume fraction is

$$\frac{\partial \alpha^d}{\partial t} + \frac{\partial}{\partial x_j}\left(\alpha^d\left[u_j + \left(1 - c^d\right)u_j^{dc}\right]\right) =$$
$$\frac{\partial}{\partial x_j}\left(D^{md}\frac{\partial \alpha^d}{\partial x_j}\right) \qquad (2)$$

The volume fraction of the dispersed phase is α^d, and the mass fraction of the dispersed phase is c^d, see Eq. (5). The j-component of the relative velocity between the dispersed and the continuous phase is $u_j^{dc} = u_j^d - u_j^c$. The use of superscripts to denote phase must not be confused with tensor notation. In

the present work, the turbulent diffusion constant is expressed

$$D^{md} = \nu + D_t^d \nu_t + D_{\text{VOF}} \left(\frac{6}{\pi} \frac{\alpha}{\alpha_{\max} - \alpha} \right)^{1/3} |\vec{u}^{dc}| d \quad (3)$$

The kinetic viscosity of the mixture is $\nu = \mu/\rho$, where μ is the dynamic viscosity. The eddy viscosity $\nu_t = \mu_t/\rho$ will be defined below. The value of the diffusion constant applied here is $D_t^d = 1.2$, based on numerical experiments on turbulent diffusion of a scalar by Moraga et al. (2001). The third term on the right hand side of Eq. (3) was included in the model to avoid unrealisticly high volume fractions of the disperse phase. The term is composed of a constant D_{VOF}, which is of order one, the approximate distance between two bubbles, $\left(\frac{6}{\pi} \frac{\alpha}{\alpha_{\max} - \alpha} \right)^{1/3}$, the realtive velocity and the bubble diameter d. The momentum equation is

$$\frac{\partial}{\partial t} (\rho u_i) + \frac{\partial}{\partial x_j} (\rho u_j u_i) = -\frac{\partial p}{\partial x_i}$$
$$+ \frac{\partial}{\partial x_j} \left([\mu + \mu_t] 2S_{ij} \right) + \rho g_i - \frac{\partial}{\partial x_j} \left(\rho c^c c^d u_i^{dc} u_j^{dc} \right) \quad (4)$$

Here, p is the mixture pressure, the shear rate is $S_{ij} = \frac{1}{2} (\partial u_i/\partial x_j + \partial u_j/\partial x_i)$, and g is the acceleration of gravity. The mixture properties are defined by

$$\rho = \sum_{k=1}^{2} \alpha^k \rho^k \quad (5)$$

$$u_i = \frac{1}{\rho} \sum_{k=1}^{2} \alpha^k \rho^k u_i^k = \sum_{k=1}^{2} c^k u_i^k \quad (6)$$

which also defines the mass fraction c^k of phase k. The phase indices 1 and 2 correspond to either disperse or continuous phase.

Sub-grid turbulence model

The LES model requires numerical resolution of the energetic range of turbulent eddies, while the small scale turbulence is accounted for by an eddy viscosity. Here, we apply the Smagorinsky (1963) model for the eddy viscosity:

$$\nu_t = C_S^2 \Delta^2 |S| \quad (7)$$

The magnitude of the shear rate is $|S| = \sqrt{S_{ij} S_{ij}}$. The Smagorinsky constant was chosen to be $C_S = 0.2$ in the present study. This value is taken from a

theoretical analysis by Lilly, see Rogallo and Moin (1984), where it is assumed that the length-scale of the mesh increment is in the inertial sub-range, so that the model spectrum due to Kolmogorov can be applied. The conventional value of the constant for single phase flow is between 0.11 and 0.15.

The relative velocity

Two different models for the motion of the bubbles relative to the liquid were applied in the present study. The first model applied a constant relative velocity. For bubbles in the size range observed in the experiments by Becker et al. (1999), i.e. a diameter close to 5 mm, the relative velocity is approximately constant and equal to the terminal velocity U_T of a single bubble:

$$\left(u^{dc}, v^{dc} \right) = (0, U_T) \quad (8)$$

This is a reasonable approximation for single bubbles with Eotvos number in the range 0.4 to 40. For air bubbles in water, this corresponds to diameters in the range 1.5 to 20mm, see Grace (1973) for details. The terminal velocity was chosen to be $U_T = 0.2$ m/s, as in Sokolichin and Eigenberger (1999).

Alternatively, the relative velocity of a single bubble can be computed from Newton's 2nd law, assuming equilibrium and including forces due to drag, buoyancy and lift, respectively:

$$\begin{aligned} 0 = \quad & \frac{1}{2} \rho^c C_D |u_i^{dc}| u_i^{dc} \frac{\pi}{4} d^2 && \text{Drag force} \\ + \quad & m^c \left(1 - \frac{\rho^d}{\rho^c} \right) g_i && \text{Gravity force} \\ + \quad & m^c C_L \left(\vec{u}^{dc} \times \vec{\omega}^c \right)_i && \text{Lift force} \end{aligned} \quad (9)$$

Here, m^c is the mass of a spherical volume of the continuous phase with diameter d. The relative velocity can then be solved iteratively from the equation

$$u_i^{dc} = \frac{4 \, d \, a_i}{3 \, C_D |u_i^{dc}|^0} \quad (10)$$

where the superscript 0 denote the previous iteration, and $a_i = -(1 - \rho^d/\rho^c)g_i - C_L(\vec{u}^{dc} \times \vec{\omega}^c)_i$ is the ith component of the acceleration due to gravity and lift. The drag coefficient for bubbles can be formulated

$$C_{D,0} = \max \left[C_{D,\text{sphere}}, C_{D,\text{bubble}} \right] \quad (11)$$

The drag coefficient for a sphere was compiled by Morsi and Alexander (1972):

$$C_{D,\text{sphere}} = \begin{cases} 24/\text{Re} & \text{if} \quad \text{Re} < 0.1 \\ 1/\text{Re}(22.73 + 0.0903/\text{Re} + 3.690\text{Re}) & \text{if} \quad \text{Re} < 1 \\ 1/\text{Re}(29.1667 - 3.8889/\text{Re} + 1.222\text{Re}) & \text{if} \quad \text{Re} < 10 \\ 1/\text{Re}(46.50 - 116.67/\text{Re} + 0.6167\text{Re}) & \text{if} \quad \text{Re} < 100 \\ 1/\text{Re}(98.33 - 2778/\text{Re} + 0.3644\text{Re}) & \text{if} \quad \text{Re} < 1000 \\ 1/\text{Re}(148.62 - 47500/\text{Re} + 0.357\text{Re}) & \text{if} \quad \text{Re} < 5000 \\ 1/\text{Re}(-490.546 + 578700/\text{Re} + 0.46\text{Re}) & \text{if} \quad \text{Re} < 10000 \\ 1/\text{Re}(-1662.5 + 5416700/\text{Re} + 0.5191\text{Re}) & \text{if} \quad \text{Re} > 10000 \end{cases} \tag{12}$$

The bubble Reynolds number is $\text{Re} = \rho|u^{dc}|d/\mu$. The drag coefficient for a spherical cap bubble was proposed by Johansen and Boysan (1988)

$$C_{D,\text{bubble}} = \frac{0.622}{1/\text{Eöt} + 0.235} \tag{13}$$

The Eötvos number is $\text{Eöt} = (\rho^c - \rho^d)gd^2/\sigma$. The hindered settling effects was introduced via the empirical formula proposed by Rusche and Issa (2000):

$$C_D = C_{D,0}f(\alpha) \tag{14}$$
$$f(\alpha) = \exp K_1\alpha + \alpha^{K_2} \tag{15}$$

where $K_1 = 3.64$ and $K_2 = 0.864$ for bubbles. The drag coefficient $C_{D,0}$ is the derived from Eq. (11) and is valid for small volume fractions α.

The lift force acting on bubbles at various Eöt was investigated by Tomiyama (1998):

$$C_L = \begin{cases} \min\left[0.288\tanh\left(0.121\text{Re}\right),\right. \\ \quad \left.0.00105\text{Eöt}^3 - 0.0159\text{Eöt}^2 - 0.0204\text{Eöt} + 0.474\right] & \text{if} \quad \text{Eöt} < 4 \\ 0.00105\text{Eöt}^3 - 0.0159\text{Eöt}^2 - 0.0204\text{Eöt} + 0.474 & \text{if} \quad 4 \leq \text{Eöt} \leq 10 \\ -0.29 & \text{if} \quad \text{Eöt} > 10 \end{cases} \tag{16}$$

The coefficient is positive for small Eöt and becomes negative for deformed bubbles. In the present study, $C_L = 0.11$ was applied, corresponding to Eöt $= 5$. The virtual mass force was not considered in the present work.

Further model assumptions

The viscosity of the mixture is modeled by the equation given by Ishii and Mishima (1984)

$$\mu = \mu^c\left(1 - \frac{\alpha}{\alpha_{\max}}\right)^{-2.5\alpha_{\max}\mu^*} \tag{17}$$
$$\mu^* = \frac{\mu^d + 0.4\mu^c}{\mu^d + \mu^c} \tag{18}$$

For the present cases, the viscosity is mostly similar to the continuous phase viscosity.

Results

This section first compares the conventionally applied $k\epsilon$ turbulence model with the $k\omega$ model and the LES models described in section . The cur-

SIMULATION

Implementation

The model given by Eq. (1) - (4) was implemented especially for the present work in the commercial CFD code Fluent 6.1.22, see Fluent User's Guide (2003), as user-defined functions (udf). Fluent was run as for single-phase flow. An additional transport equation for the disperse volume fraction, source terms in the mass and momentum equations, as well as computation of physical properties, were implemented especially for the present study via udf. The simulations presented here applied the QUICK interpolation scheme for convective terms and 2nd order implicit time stepping.

Case description

The meshes were generated with uniform spacing. The number of cells are given in table 1. The density of the continuous phase was 998 kgm^{-3}, the density of the disperse phase was 1.23 kgm^{-3}, the viscosity of the continuous phase was 0.001 Pa.s.

rent three-dimensional simulations are compared to two-dimensional simulations of the same case and experimental results by Pfleger et al. (1999).

The transient behavior of the flow was monitored by recording the viscous force $F_D = \tau_w A_m$ acting

Case	$N/1000$	Model	d [mm]	u^{dc}	D_t	D_{VOF}	T [s]
A1	36	$k\epsilon$	5	0.2	1.2	0.5	11.3 ± 0.1
A2	36	$k\omega$	5	0.2	1.2	0.5	10.7 ± 0.2
A3	36	Smagorinsky	5	0.2	1.2	0.5	13.0 ± 1.0
A4	36	Smagorinsky	6	Eq. (10)	0	0	11.8 ± 0.2
B1	171	Smagorinsky	5	0.2	1.2	0.5	12.2 ± 0.4
B2	171	Smagorinsky	6	Eq. (10)	0	0	11.7 ± 0.4

Table 1: Case description. N denotes number of control volumes, T denotes period of oscillation, to be described in section

on a small area A_m of the sidewall, shown in figure 2. The area of the monitoring area was 10^{-4} m^2. The drag coefficient was

$$C_D = \frac{F_D}{1/2\rho^c U_T^2 A_m} \qquad (19)$$

where U_T is defined in Eq. (8).

Comparison of turbulence models

Figure 3 display the drag coefficient Eq. (19) as a function of time for the coarse mesh cases. The absolute value of the time along the axis is not of importance, because the various cases was started at different absolute times. The figures show the behavior over a time span of 200 s, or approximately 18 periods of oscillations. Case A1 exhibits large time scale fluctuations, while the other cases show higher frequencies. The relatively high effective viscosity produced by the $k\epsilon$ method tends to damp higher frequencies. The period of oscillation was computed applying Fast Fourier Transform. The results are given in the last column of table 1. For the coarse mesh cases, the variation in oscillation period was close to 10 %. The uncertainty in the period was relatively small, except for case A3. Figure 4 displays the qualitative difference between the different models. Case A1, exhibited a relatively thick bubble plume due to the high magnitude of the turbulent viscosity. With case A2, the plume was more narrow, and with the LES model, cases A3 and A4 gave a fragmented gas plume. In spite of the qualitative difference between case A1 and the other coarse mesh cases, however, the period of oscillation was similar.

Comparison with two-dimensional case and experimental data

In figure 5, the case A3 is compared with experimental data and a 2D simulation. The present results were obtained from averaging 200 flow fields spanning a time period of 100 s (approximately 8.5 periods of plume oscillation). As can be seen from the asymmetry of the curves with respect to the centerline, the number of samples was not sufficient. Comparing the magnitude of the computed

and measured velocity, the agreement is approximately within the experimental error. Case A3 showed somewhat better agreement with the experiments in the qualitative sense, because the velocity peaks were sharper than in case L3. The deviation close to the column walls was discussed in the previous paper Bech (2005).

Phase averaging of velocity

In order to analyze the turbulence field properly, one can apply phase, or conditional, averages of the flow filed to obtain an ensemble average of the flow variables that corresponds to a specific phase of the oscillating motion. Assuming a period of 12 s, a time span of 252 s was analyzed for case A4. Eleven phases were chosen, and 21 flow fields were averaged for each phase. The phase averaged velocities are depicted in figure 6. In the sequence of figures, one can follow large-scale vortices moving downwards, similar to figure 1. The large-scale structures from the simulation are not very distinct (it was not possible to achieve better graphical resolution in this print).

Discussion and further work

Becker et al. (1999) applied a bubble column with thickness 0.04 m, equipped with a single-orifice sparger. The gas rate was 0.8 l/min, corresponding to a superficial gas velocity of 0.17 cm/s. The period of plume oscillation, T, was measured to be between 16 and 19 s. Buwa and Ranade (2002) measured the period of oscillation for various conditions. For a superficial gas velocity of 0.17 cm/s and with a sparger consisting of a rectangular array of holes, the result was $T \simeq 12.2$ s. The period was not significantly dependent on the sparger design. The main differences between the two experimental investigations were the lateral width of the column, which was 5 cm in the latter work, as well as the sparger geometry. The present results agree with the latter experimental investigation.

Attempts to make conditional averages, or phase-averages, of the bubble plume, turned out to give a 'blurred' image of the plume oscillation. This may be caused by the spectrum of higher frequency

oscillations, or that the fluctuations actually deviated from periodic motion. Both arguments can be supported by experimental evidence, in particular the fact that different measurements of the oscillation period disagree. The experimental signal reproduced by Buwa and Ranade (2002) (their figure 2) resembles the signal derived from LES type simulations, and not the regular signals obtained with the $k\epsilon$ model. One problem about generating good phase averages is related to data storage. In the present work, the flow field was sampled every 0.5 s. If a better accuracy for the oscillating period is needed, more samples must be taken. An alternative approach is to run the simulations for several more hundred seconds and apply conditional averaging, i.e. make a sample when a special event occurs in the flow field. Further work will look into these possibilities.

Two different models for the bubble relative velocity were applied in the present study (case A3 and A4). The differences in the computed flow fields have not been analyzed due to the non-conclusive study of phase averages. From animations of the flow field, it can be seen that the lift force causes the plume to split and become more unstable in the case with $C_L \neq 0$, i.e. case A4. This behavior can be recognized in figure 4.

References

Bech, K., 2005. Dynamic simulation of a 2d bubble column. To appear in Chem. Eng. Sci.

Becker, S., De Bie, H., Sweeney, J., 1999. Dynamic flow behaviour in bubble columns. Chem. Eng. Sci. 54, 4929–4935.

Becker, S., Sokolichin, A., Eigenberger, G., 1994. Gas-liquid flow in bubble columns and loop reactors: Part ii. comparison of detailed experiments and flow simulations. Chem. Eng. Sci. 49 (24B), 5747–5762.

Buwa, V. V., Ranade, V. V., 2002. Dynamics of gas-liquid flow in a rectangular bubble column: Experiments and single/multi-group cfd simualtions. Chem. Eng. Sci. 57, 4715–4736.

Deen, N., Solberg, T., Hjertager, B., 2001. Large eddy simulation of the gas-liquid flow in a square-sectioned bubble column. Chem. Eng. Sci. 56, 6341–6349.

Fluent User's Guide, 2003. Fluent 6.1 User's guide. Fluent Inc., New Hampshire.

Grace, J., 1973. Shapes and velocities of bubbles rising in infinite liquids. Trans. Instn. Chem. Engrs. 51, 116–120.

Ishii, M., Mishima, K., 1984. Two-fluid model and hydrodynamic constitutive relations. Nucl. Eng. and Des. 82, 107–126.

Johansen, S. T., Boysan, F., 1988. Fluid dynamics in bubble stired ladles. Met. Trans. B 19, 755–764.

Moraga, F. J., Larreteguy, A. E., Drew, D., Jr., L. R., 2001. Asessment of turbulent dispersion models for bubbly flows. In: Matsumoto, Y., Sommerfeld, M., Stock, D. (Eds.), 4th International Congress on Multiphase flows.

Morsi, S., Alexander, A., 1972. An investigation of particle trajectories in two-phase flow systems. J. Fluid Mech. 55, 193–208.

Oey, R., Mudde, R., van den Akker, H., 2003. Sensitivity study on interfacial closure laws in two-fluid bubbly flow simulations. AIChE J. 49 (7), 1621–1636.

Pfleger, D., Becker, S., 2001. Modelling and simulation of the dynamic flow behaviour in a bubble column. Chem. Eng. Sci. 56, 1737–1747.

Pfleger, D., Gomes, S., Gilbert, N., Wagner, H., 1999. Hydrodynamic simulations of laboratory scale bubble columns fundamental studies of eulerian-eulerian modelling approach. Chem. Eng. Sci. 54, 5091–5099.

Rogallo, R., Moin, P., 1984. Numerical simulation of turbulent flows. Ann. Rev. Fluid Mech. 16, 99–137.

Rusche, H., Issa, R., 2000. The effect of voidage on the drag force on particles, droplets and bubbles in dispersed two-phase flow. In: 2nd Japanese-European Two-Phase Flow Meating. Tsukuba, Japan.

Smagorinsky, J., 1963. General circulation experiments with the primitive equations. i. the basic experiment. Mon. Weather Rev. 91, 99–164.

Sokolichin, A., Eigenberger, G., 1999. Applicability of the standard k-e turbulence model to the dynamic simulation of bubble columns: Part i. detailed numerical simulations. Chem. Eng. Sci. 54, 2273–2284.

Takeda, H., Esaki, N., Doi, K., Murakami, H., Yamasaki, K., Kawase, Y., 2004. Flow simulation in bubble columns in regard to bubble coalescence and break-up utilizing les and dem. J. Chem. Eng. Japan 37 (8), 976–9891.

Tomiyama, A., 1998. Struggle with computational bubble dynamics. In: Third international conference on multiphase flows. Lyon, France.

Troshko, A., Hassan, Y., 2001. A two-equation turbulence model of turbulent bubbly flows. Int. J. Multiphase flow 27, 1965–2000.
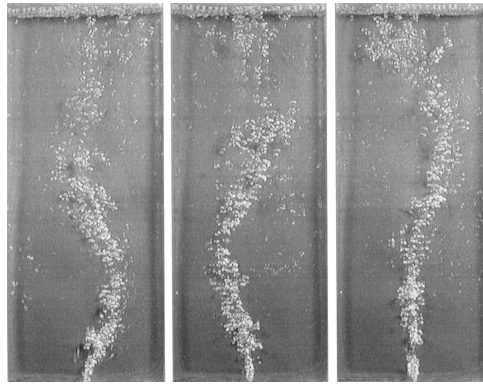
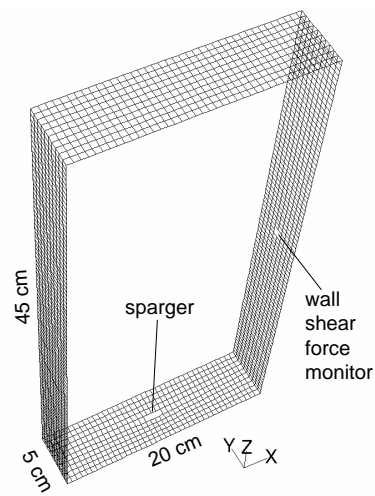Figure 1: Visualization of meandering bubble plume from Becker et al. (1999).

Figure 2: Geometry of rectangular column. The mesh shown on the side walls corresponds to the coarse mesh cases A1-A4.
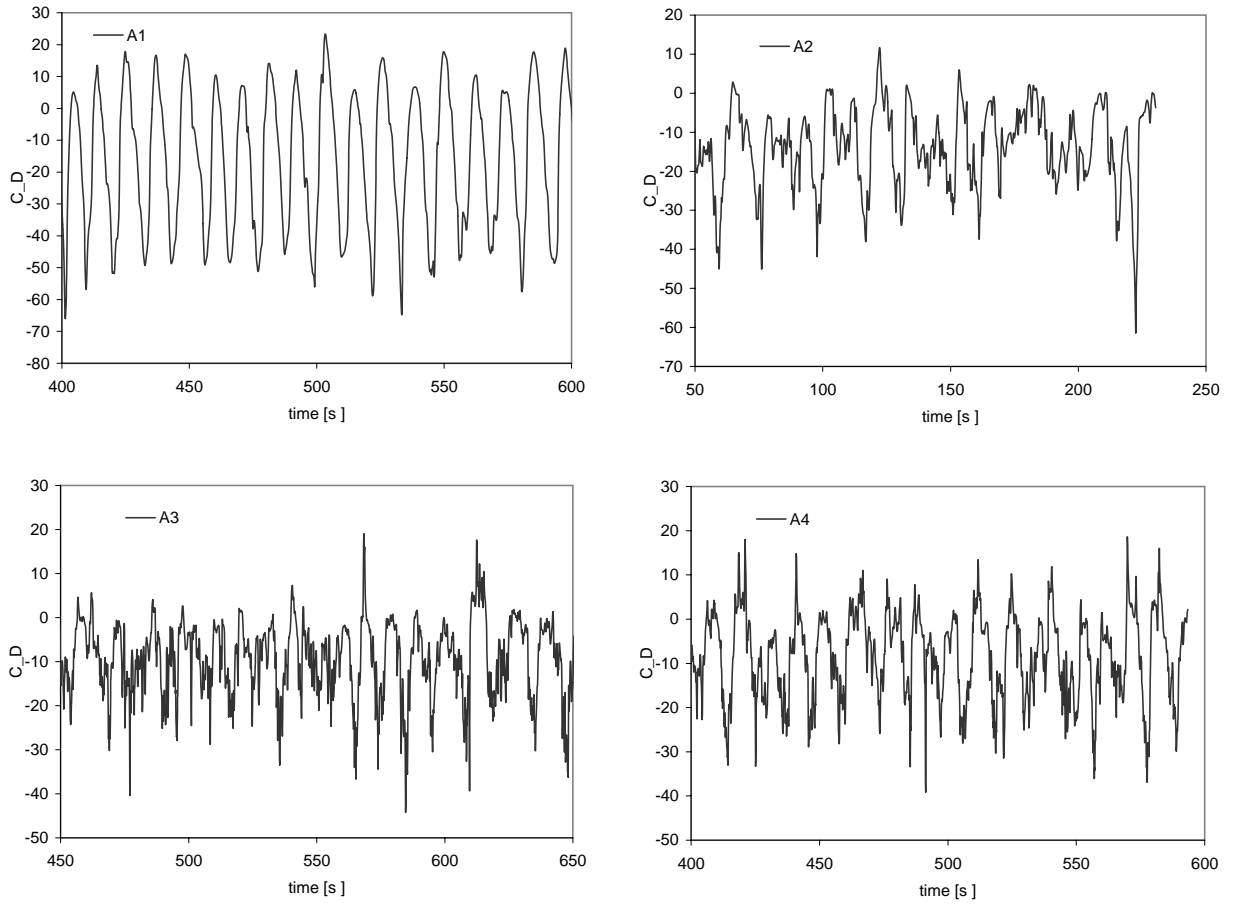
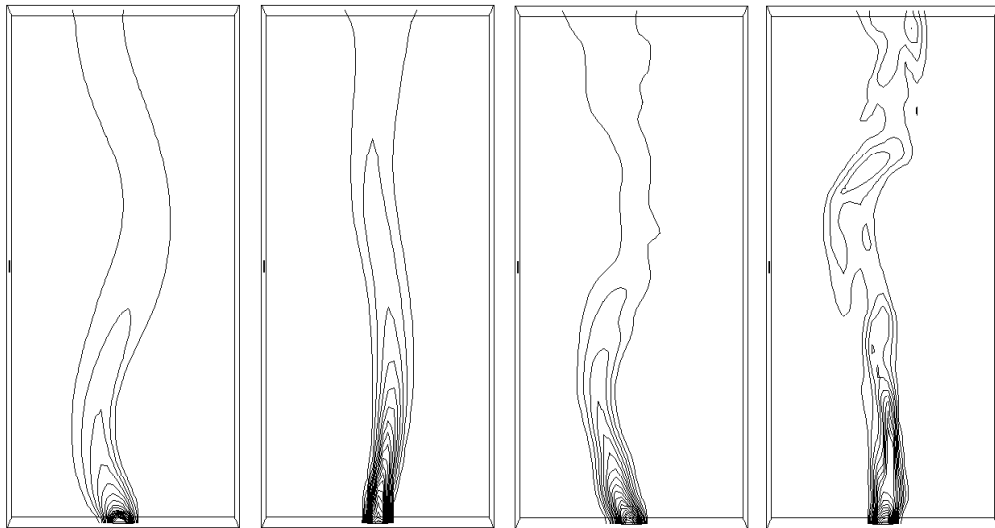Figure 3: The drag force coefficient versus time for the coarse mesh cases A1-A4.

Figure 4: Contours of gas volume fraction (0 to 0.2) for case A1-A4 from left to right. The instantaneous views have been chosen arbitrarily.
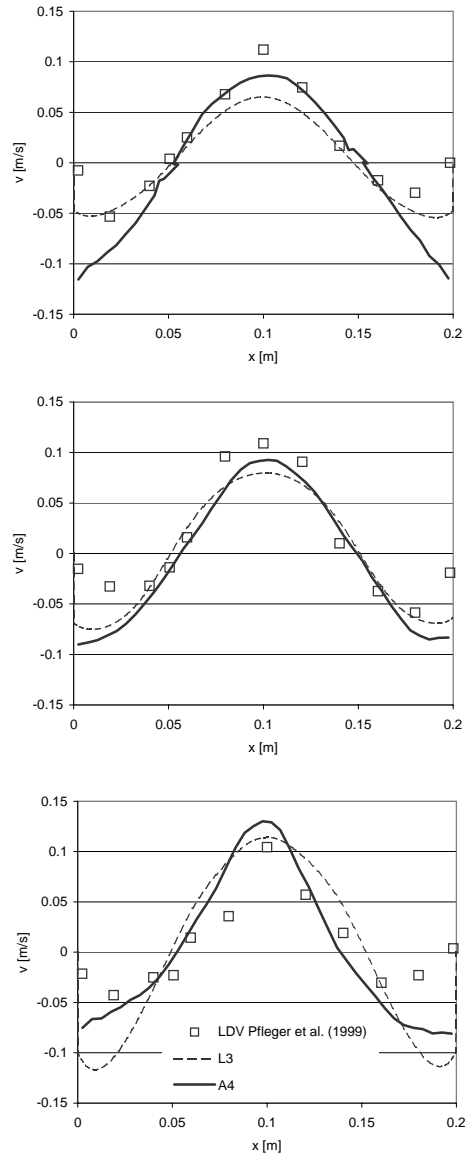
7

Figure 5: Time-averaged velocity at positions 13, 25 and 37 cm above sparger. Experimental data, present case A4 and case L3 from Bech (2005) are shown. The latter case was 2D and applied a mixing length turbulence model.
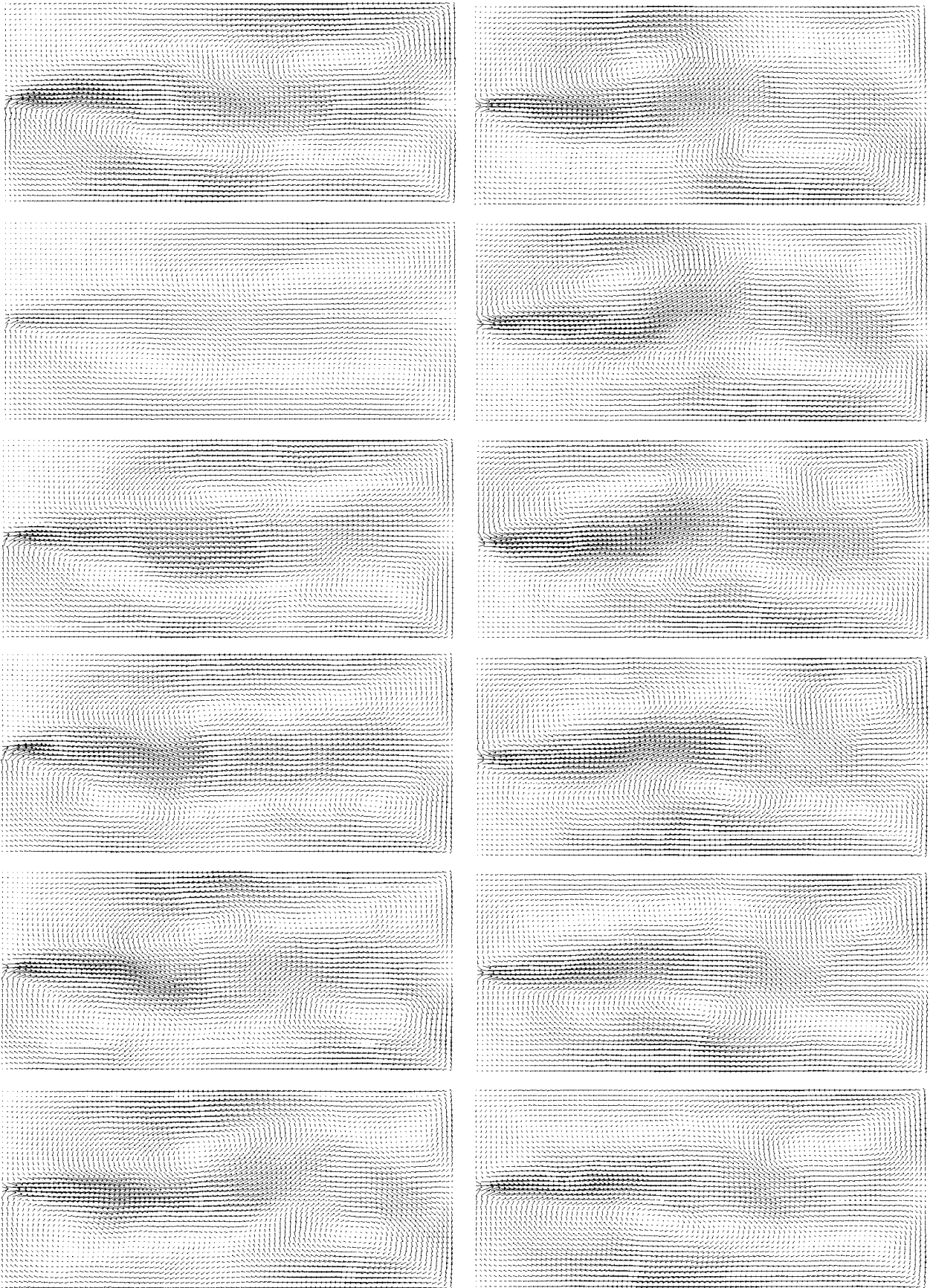
Figure 6: Velocity vectors for case A4, time interval between each figure is 1 s. The figure must be viewed with the left margin pointing downwards. The series starts in the upper left corner, then continues to the right, to the the lower left corner and to the right. The vectors are shown the middle plane, the magnitude varies between 0 and 0.2 m/s.